REGULAR PAPERS

Experimental investigation of the effect of signal reflection and coverage area on indoor acoustical positioning using transponders with adaptive signal level normalizer

Japanese Journal of Applied Physics **57**, 07LC03 (2018)
https://doi.org/10.7567/JJAP.57.07LC03

REGULAR PAPER

Experimental investigation of the effect of signal reflection and coverage area on indoor acoustical positioning using transponders with adaptive signal level normalizer

Hirokazu Iwaya[1], Koichi Mizutani[1,2]*, Tadashi Ebihara[1,2], and Naoto Wakatsuki[1,2]

[1]*Graduate School of Systems and Information Engineering, University of Tsukuba, Tsukuba, Ibaraki 305-8573, Japan*
[2]*Institute of Engineering Mechanics and Systems, University of Tsukuba, Tsukuba, Ibaraki 305-8573, Japan*

*E-mail: mizutani@iit.tsukuba.ac.jp

Received November 6, 2017; accepted January 18, 2018; published online June 1, 2018

Acoustical positioning is one of the attractive schemes for indoor positioning. To achieve positioning with a small number of devices, we have proposed a transponder-based scheme using audible sound. However, this scheme has not yet been evaluated in an actual large-scale environment. In addition, the effects of signal reflection were not revealed. In this study, the proposed scheme is evaluated in a large-scale room, and the effects of signal reflection and coverage positioning area are investigated. The experimental results suggest that the proposed method is sensitive to signal reflections. To cope with this problem, we improved the measurement procedure to detect a direct signal. It was found that the improved scheme can achieve positioning with error of less than 0.08 ± 0.01 m covering a 7×7 m^2 area. Hence, we confirmed that the improved method can achieve accurate positioning and can cover a large-scale area. © 2018 The Japan Society of Applied Physics

1. Introduction

An indoor positioning system can achieve large-scale area navigation, evacuation guide system, and robot automation. Various measurement techniques are available for indoor positioning, such as the use of acoustical waves,[1–24] laser light,[25] radio waves,[26] magnetic force, and acceleration force.[27] Among them, the use of acoustical waves has advantages in terms of cost effectiveness and positioning accuracy. Moreover, the acoustical indoor positioning system can utilize existing acoustical infrastructures, such as loudspeakers installed for announcements in a building or a subway concourse as anchors and smartphones with a microphone and a loudspeaker as terminals.

In general, indoor acoustical positioning is performed as follows: (1) measurement of the time of flight (TOF) of acoustical signals and (2) position estimation using multiple information, such as TOFs and position of known signal sources (anchors). The use of TOF is common in positioning and other diverse fields such as biomedical measurement,[1,2] posture and velocity measurement,[1–23] nondestructive inspection,[28–35] and thermal environment measurement.[36–42]

Ultrasound-based indoor positioning is suitable for small-scale area positioning in a corridor or room. However, this method cannot simply be applied to a large-scale environment such as a building or a subway concourse, since a large number of ultrasonic sensors (anchors) are required to cover such a wide area because ultrasounds attenuate rapidly with increasing frequency. In addition, clock synchronization among a terminal and multiple anchors is required to achieve accurate positioning, resulting in an increase in system complexity.

To cope with this problem, we have proposed a transponder-based acoustical positioning method using audible sound.[43] The proposed method has several advantages over existing ultrasound positioning methods: (i) audible sound can cover a large-scale area compared with ultrasound and (ii) the proposed method does not require complex clock synchronization for the measurement of TOF by introducing a transponder-based system. Furthermore, an adaptive signal level normalizer enables the system to measure multiple TOFs by adjusting the signal-to-noise ratio (SNR) of each signal equally. In a previous study, we evaluated the performance of the proposed system in an ideal environment, i.e., an anechoic chamber, and we found that the proposed method achieved a positioning error of 0.08 ± 0.02 m.[43] However, the performance of the proposed method has not yet been evaluated in an actual environment. In an actual environment, the effect of signal reflection (e.g., the transmitted signal from anchors will propagate to a terminal in direct and floor-reflected paths) worsens the positioning accuracy. In addition, the coverage area of the system has not yet been revealed.

The purpose of this study is to investigate the performance of the transponder-based indoor acoustical positioning system in an actual indoor environment, and to clarify the coverage area of the system. We deployed the proposed system in a room, and confirmed the effect of signal reflection. In addition, we improved the conventional system, and revealed the coverage area of the system. This paper consists of 5 sections. In Sect. 2, we explain our conventional proposed method. In Sect. 3, we describe experiments conducted using the conventional positioning method in a large-scale area. In Sect. 4, we discuss the effect of signal reflection, the improved peak detection method, and the conducted experiments. In Sect. 5, we conclude this work.

2. Measurement principle of transponder-based acoustical positioning

An overview of the proposed method is shown in Fig. 1. This method consists of an arbitrarily located terminal and fixed multiple transponders #i ($i = 1, 2, 3$) on a ceiling. The proposed method measures round-trip TOFs among the terminal and multiple transponders. Then, the terminal calculates its position by combining the measured TOFs and known transponder positions.

2.1 Measurement of round-trip TOF

The block diagram of the measurement procedure of TOF is shown in Fig. 2. First, the terminal transmits a request signal to each transponder at $t_{\mathrm{T}i}$. The signal is modulated by a specific maximum-length sequence (M-sequence) and the carrier frequency f_{C}. Because the M-sequence has a good

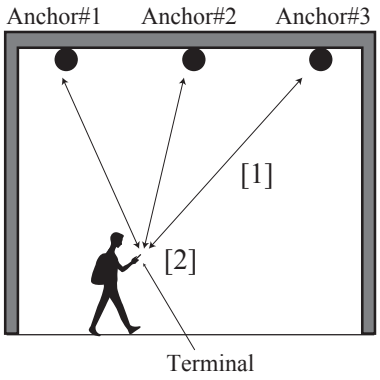

Fig. 1. Overview of proposed positioning method:[1)] TOF measurement and[2)] the terminal calculates position by using TOFs (distances) and anchor positions.

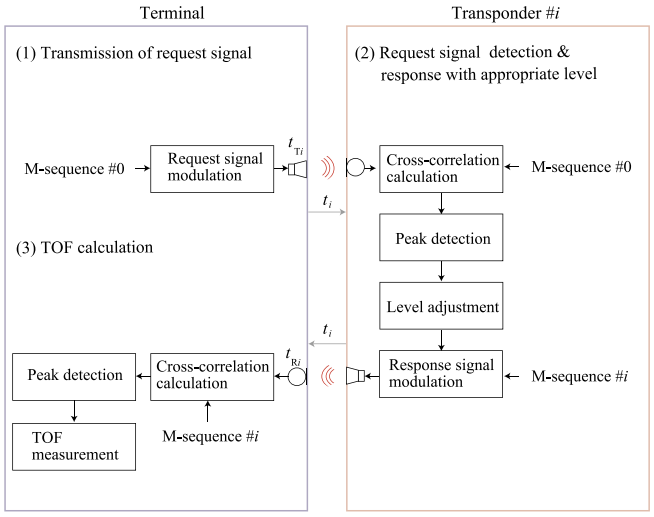

Fig. 2. (Color online) Block diagram of measurement procedure of TOF.

auto-correlation property, it enables us to easily measure TOF from the maximal peak location in the cross-correlation function of transmitted and received signals.[6,11,15,16,21–24)] Second, transponder #*i* receives the request signal. Each transponder has a replica of the M-sequence #0 and the unique #*i* M-sequence. They detect the request signal when the maximal peak value in the cross-correlation function between the received and the replica signal exceeds a threshold value. Then, the transponder adjusts the appropriate response signal level by using the maximal peak value in the cross-correlation function for gain control. After a constant delay time w, each transponder transmits a response signal. Third, the terminal, which also has all of the replica M-sequences, receives the response signal and calculates the round-trip TOF between the terminal and the transponder at $t_{\mathrm{R}i}$. The round-trip TOF of t_i can be determined using the multiple-transponder response signal:

$$t_i = \frac{t_{\mathrm{R}i} - t_{\mathrm{T}i} - w}{2}. \tag{1}$$

2.2 Positioning using multiple TOFs

After the measurement of multiple TOFs among the terminal and the transponders, the terminal calculates its own position by combining the known information of transponder positions and distances among the terminal and the transponders. Assuming that the speed of sound (c) is constant, the distance between the terminal and each transponder, r_i, is

$$r_i = ct_i. \tag{2}$$

The terminal position (x, y, z) is expressed using the transponder position (x_i, y_i, z_i) and each distance r_i,

$$r_i^2 = (x_i - x)^2 + (y_i - y)^2 + (z_i - z)^2. \tag{3}$$

Because Eq. (3) is a nonlinear simultaneous equation, an iterative method such as the Newton–Raphson method is utilized to solve the equation for estimating the terminal position. If we can measure TOFs accurately, the terminal estimates its position with a few iterative steps.

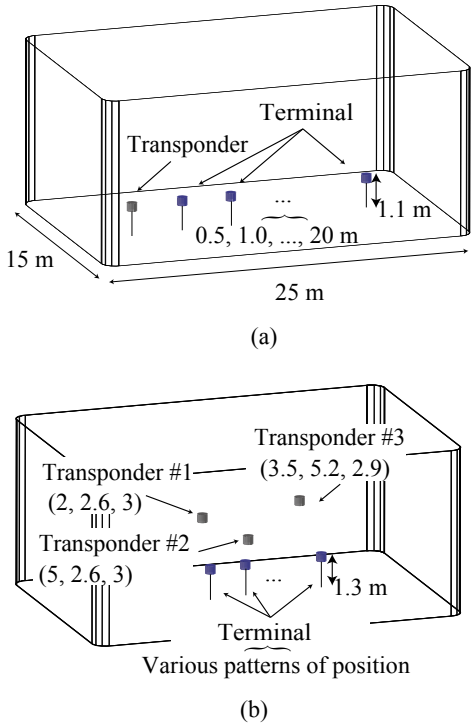

Fig. 3. (Color online) Schematic view of experiment system: (a) ranging experiment and (b) positioning experiment.

3. Experiments using conventional positioning method in a large-scale area

The performance of the proposed method was shown to be valid in an ideal environment such as an anechoic chamber.[43)] In this section, we validate the conventional positioning method in an actual environment. First, we explain our experimental setup. Second, we describe the experimental results of ranging and positioning. Finally, we discuss the results of experiments.

3.1 Experiment environment

A schematic view of the experiment system is shown in Fig. 3. Experiments were carried out in a large-scale room of 15 (W) × 25 (D) × 10 (H) m^3 size. Each of the terminal and transponders consisted of an omnidirectional microphone (MIC; DB Products c9767), a loudspeaker (SP; Fostex P-650K), an analog-to-digital (A-D)/digital-to-analog (D-A) converter (National Instruments USB-6221 or 6259), and a personal computer. They were controlled via measurement software (National Instruments LabVIEW). The generated signals were also calculated by using a numerical computing

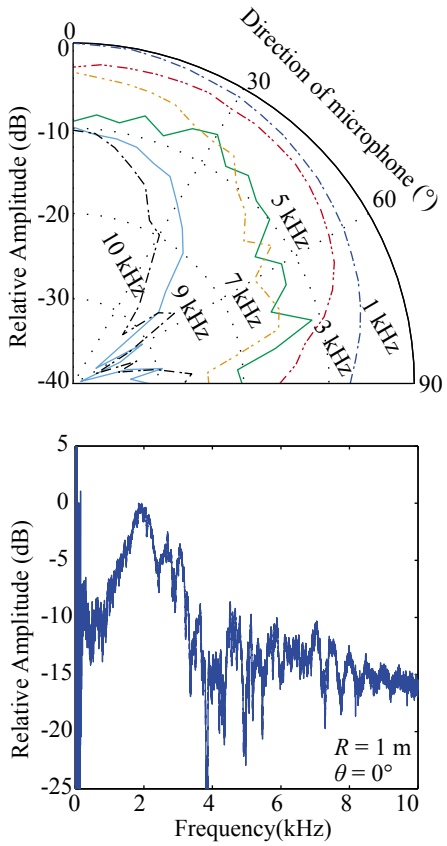

Fig. 4. (Color online) Directivity and frequency characteristics of MIC and SP.

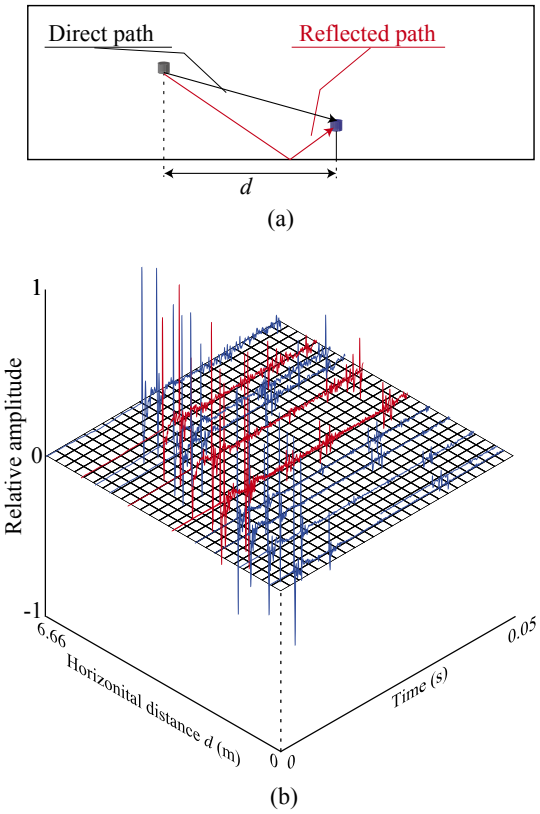

Fig. 5. (Color online) Impulse responses between the terminal and the transponder: (a) direct path and reflected path, (b) examples of impulse responses (blue: direct signal exceeds the reflected signal; red: reflected signal exceeds the direct signal).

tool (Mathworks MATLAB). The sampling frequency of the A-D/D-A converter was 50 kHz. The signals had the carrier frequency (f_C) of 5 kHz, bandwidth of ±5 kHz, and length of 25.4 ms. The feedback tap of the M-sequence was of the 7th order and consists of 127 chips. We set the chip time as 0.2 ms. In the ranging experiments, we utilized the feedback tap for the $(7, 5, 4, 3, 2, 1, 0)$ M-sequences #0 and #i. In the positioning experiments, we utilized $(7, 1, 0)$ for the terminal. In addition, we used $(7, 5, 4, 3, 2, 1, 0)$, $(7, 3, 0)$, and $(7, 3, 2, 1, 0)$ for transponder#1, transponder#2, and transponder#3, respectively. Note that the above M-sequences include preferred pairs to minimize the interference among these sequences. The above parameters were also utilized in our previous study.[43)] In each position indicated in Fig. 3, round-trip TOFs were measured 10 times. The directivities of MIC and SP were measured at various directions from 0 to 90° at 5° steps. The frequency response was measured by using an up-chirp signal (5 Hz to 20 kHz, 1 m, $\theta = 0°$). The results are shown in Fig. 4. As shown in this figure, the signal within 10 kHz was valid for the measurements. Therefore, we chose the carrier frequency of 5 kHz.

In this experimental environment, there are two signal paths between the terminal and the transponder: direct path and reflected path [Fig. 5(a)]. In Fig. 5(a), d is the horizontal distance between the terminal and the transponder. To verify this assumption, we measured the impulse response of the room. Examples of impulse responses are shown in Fig. 5(b). In this environment, the reverberation time was about 0.9 to 1.0 s, regardless of d. In Fig. 5(b), the blue line shows the case in which the position where the peak is maximum corresponds to the TOF of the direct signal, and the red line shows the case in which the position where the peak is maximum corresponds to the TOF of the reflected signal. As shown in this figure, as the distance d increases, the probability that the peak value of the reflected signal exceeds that of the direct signal increases.

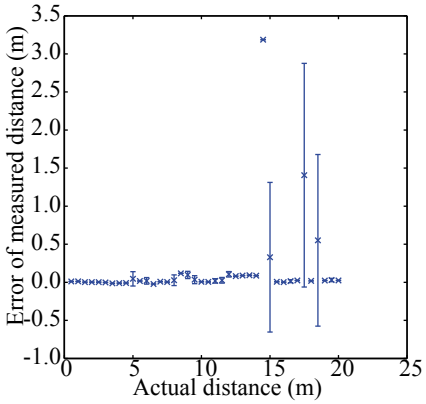

Fig. 6. (Color online) Ranging result obtained using maximal peak detection.

3.2 Experiments using conventional method

A ranging experiment was performed by changing the position of the terminal from 0.5 to 20.0 m (every 0.5 m). In each position, the positioning was performed 10 times. The result of ranging experiments is shown in Fig. 6. The measurements over 10 m distance were inaccurate. The

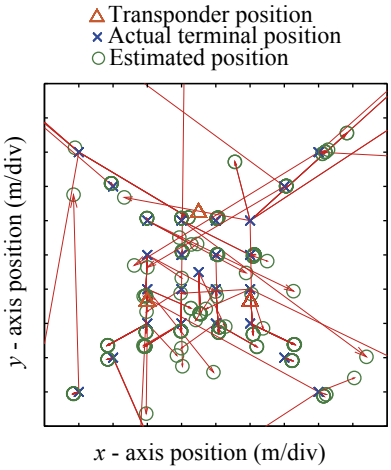

Fig. 7. (Color online) Positioning result obtained using maximal peak detection.

average error and standard deviation were 0.16 ± 0.10 m. In principle, the maximal peak detection (MPD) can detect an actual TOF. However, as shown in Fig. 5(b), the probability that the peak value of the reflected signal exceeds that of the direct signal increases. This environmental effect sometimes causes errors, as shown in Fig. 6.

A positioning experiment was performed by changing the position of the terminal in 25 patterns. In each position, the positioning was performed 10 times. The result of the positioning experiment using the conventional method is shown in Fig. 7. The red line shows the relationship between the estimated and the actual positioning results. The average positioning error and standard deviation were 1.38 ± 2.23 m. As shown in this figure, it is considered that the error of TOF worsens the positioning accuracy. When a simultaneous response signal is received from transponders, an alternative peak detection method is also necessary.

3.3 Discussion

In the previous experiments, the MPD with the adaptive signal level normalizer[43] was successfully used. However, the total measurement accuracy of TOF was insufficient. This is caused by the problem of the measurement accuracy of the round-trip TOF. An example of a cross-correlation function between the terminal and the transponder in different environments such as an anechoic chamber and a large-scale room, is shown in Fig. 8. This figure shows the tendency of the cross-correlation function. In the anechoic chamber, the maximal peak equals the true TOF. However, in the room, the cross-correlation function has multiple peaks, and the maximal peak does not equal the true TOF. It is considered that in an actual environment, the signal reflection from the floor or wall worsens the measurement accuracy. To measure TOF accurately, the proposed method should not measure the maximal peak, but the first peak in the actual environment. In other words, the first peak exceeds the appropriate threshold level, and the transponders and terminal can measure the actual TOF.

4. Improvement of signal reflection provision in large-scale area positioning

In this section, we describe the improvement of the proposed method in the large-scale area. To achieve the accurate

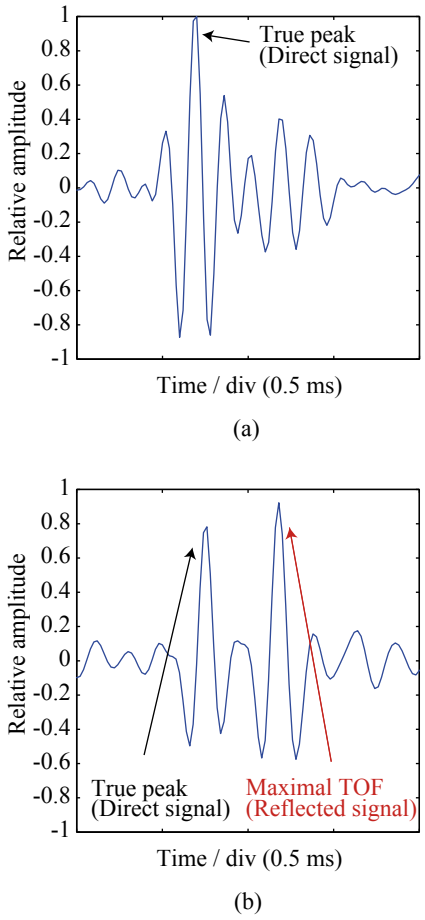

Fig. 8. (Color online) Example of cross-correlation function: (a) anechoic chamber and (b) room.

measurement of the round-trip TOF, we implemented the first peak detection (FPD) by using the cross-correlation function among the terminal and the transponders.

4.1 Improvement of TOF measurement

On the basis of the discussion in Sect. 3.3, we improved the TOF measurement procedure to detect the direct signal among numerous peaks, by focusing on the fact that the direct signal always arrives first at the receiver. The proposed FPD method detects the true TOF as follows. In the terminal, we set the threshold level as TL using the maximal peak of the cross-correlation function $C_{\max}$:

$$TL = C_{\max} \times \alpha. \tag{4}$$

If the amplitude of the peak of the cross-correlation function (which corresponds to the direct signal) exceeds TL, and that which corresponds to noise does not exceed TL, we can measure the true TOF. We assume that if the terminal can determine the appropriate threshold level, the terminal can measure TOF accurately. From experiments in a large-scale room, we found that α of 0.57 is the best to detect the true TOF. In this work, we experimentally obtained the optimal value of α, and this α should be determined carefully. In an actual environment, for example, where numerous people exist and they move randomly, this value should be updated frequently, since the sound propagation environment changes dynamically. A combination of our proposed technique and frequency-based signal processing[6,16,24] would be necessary to find and update the optimal value of α frequently.

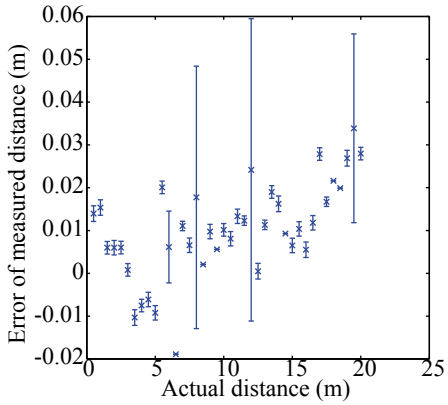

Fig. 9. (Color online) Ranging result obtained using first peak detection.

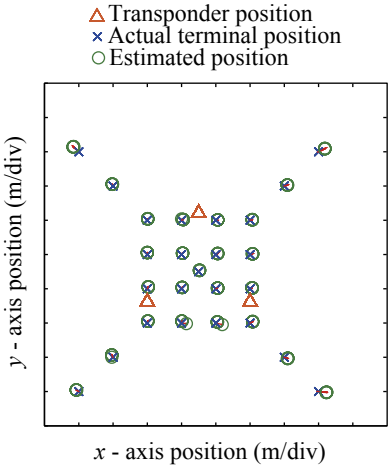

Fig. 10. (Color online) Positioning result obtained using first peak detection.

4.2 Experiments using proposed FPD method

A ranging experiment was performed by changing the position of the terminal, described in Sect. 3.2. The ranging result obtained using the FPD method is shown in Fig. 9. The average error and standard deviation were 10.2 ± 3.4 mm. As shown in this figure, the TOF can be measured accurately when the terminal is located at 0.5 to 20.0 m from the transponder.

A positioning experiment was also performed, as described in Sect. 3.2. The positioning result obtained using the FPD method is shown in Fig. 10. In all cases, the position of the terminal was accurately measured. The total terminal positioning accuracy was 0.08 ± 0.01 m within a 7×7 m^2 area. The error of the average estimated terminal position versus the distance d_c between the terminal and the center of transponders is shown in Fig. 11. This figure shows that the standard deviation is small. However, as d_c increases, the average estimated positioning error increases. The reasons for the positioning error are the directivity of the SP (Fig. 4) and the SNR among the terminal and the transponders. The directivity of the SP attenuates the SNR as d_c increases, and the terminal receives the deteriorated signal.

From the above experiment results, the FPD method can be used to measure the round-trip TOF accurately and achieve accurate positioning compared with the MPD method. The FPD method also revealed that the valid coverage area using

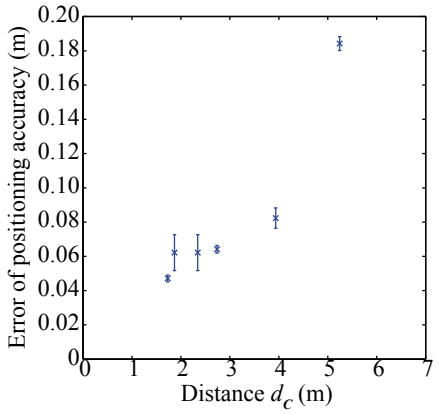

Fig. 11. (Color online) Average positioning error of estimated terminal position versus distance d_c between the terminal and the center of transponders in positioning experiment.

the proposed method was 0.08 ± 0.01 m within a 7×7 m^2 area.

5. Conclusions

The purpose of this study was to investigate the effect of the signal reflection and to evaluate the performance of the coverage positioning area by an acoustical transponder-based positioning method in an actual large-scale environment. To achieve this purpose, we investigated the effect of signal reflection and improved the measurement of round-trip TOF. In addition, we carried out experiments and revealed the coverage area by using the improved measurement method. In the ranging experiments, the proposed method can measure 10.2 ± 3.4 mm when the terminal is within 20.0 m from the transponder. In the positioning experiments, the error of the positioning accuracy was 0.08 ± 0.01 m within a 7×7 m^2 area when using three transponders as anchors. In other words, the proposed method can cover about 50 m^2 per unit. Our proposed method is expected to cover a large-scale area of over 100 m^2 efficiently by spreading and connecting units. Our future works will focus on three aspects. First is performance evaluation in the presence of an obstacle using the proposed transponder unit. Second is the introduction of the handover method in the large-scale area positioning. Third is the optimization of each transponder location.

1) K. Hoshiba, S. Hirata, and H. Hachiya, Jpn. J. Appl. Phys. **52**, 07HC15 (2013).
2) N. Thong-un, S. Hirata, and M. K. Kurosawa, Jpn. J. Appl. Phys. **54**, 07HC06 (2015).
3) J. M. Lee, D. H. Lee, H. An, N. Huh, M. K. Kim, and M. H. Lee, Proc. 30th Annu. Conf. IEEE Industrial Electronics Society, 2004, p. 448.
4) M. Inba, H. Yanagida, and Y. Tamura, Jpn. J. Appl. Phys. **47**, 3880 (2008).
5) H. Koyuncu and S. H. Yang, Proc. Int. Journal of Compututer Science and Network Security, 2010, p. 121.
6) S. Hirata and H. Hachiya, Jpn. J. Appl. Phys. **52**, 07HC06 (2013).
7) S. Hirata, L. Haritaipan, K. Hoshiba, H. Hachiya, and N. Niimi, Jpn. J. Appl. Phys. **53**, 07KC17 (2014).
8) H. Li, H. Terada, and A. Yamada, Jpn. J. Appl. Phys. **53**, 07KC18 (2014).
9) K. Zempo, T. Ebihara, and K. Mizutani, Jpn. J. Appl. Phys. **51**, 07GB09 (2012).
10) K. Zempo, K. Mizutani, and N. Wakatsuki, Jpn. J. Appl. Phys. **52**, 07HG06 (2013).
11) K. Yamanaka, S. Hirata, and H. Hachiya, Jpn. J. Appl. Phys. **55**, 07KC09 (2016).

12) C. Randell and H. Muller, Proc. Int. Conf. Ubiquitous Computing, 2001, p. 42.
13) N. Hiraoka, T. Suda, K. Hirai, K. Tanaka, K. Sako, R. Fukagawa, M. Shimamura, and A. Togari, Jpn. J. Appl. Phys. **50**, 07HC19 (2011).
14) A. Mandal, C. V. Lopes, T. Givargis, A. Haghighat, R. Jurdak, and P. Baldi, Proc. 2nd IEEE Consumer Communications Networking Conf., 2005, p. 348.
15) Y. Wang, T. Siginouchi, M. Hashimoto, and H. Hachiya, Jpn. J. Appl. Phys. **46**, 4490 (2007).
16) Y. Ikari, S. Hirata, and H. Hachiya, Jpn. J. Appl. Phys. **54**, 07HC14 (2015).
17) H. Hashizume, A. Kaneko, Y. Sugano, K. Yatani, and M. Sugimoto, Proc. IEEE Region 10 Conf. (TENCON), 2005, p. 1.
18) Y. Asakura, K. Okubo, and N. Tagawa, Jpn. J. Appl. Phys. **56**, 07JC14 (2017).
19) R. Mautz, Geod. Kartogr. **35**, 18 (2009).
20) Y. Fukuju, M. Minami, H. Morikawa, and T. Aoyama, Proc. WSTFEUS, 2003, p. 53.
21) S. Hirata and M. K. Kurosawa, Ultrasonics **52**, 873 (2012).
22) S. Hirata, M. K. Kurosawa, and T. Katagiri, IEICE Trans. Fundam. Electron. Commun. Comput. Sci. **E91-A**, 1031 (2008).
23) S. Hirata, M. K. Kurosawa, and T. Katagiri, Acoust. Sci. Technol. **30**, 429 (2009).
24) S. Widodo, T. Shiigi, N. Hayashi, H. Kikuchi, K. Yanagida, Y. Nakatsuchi, Y. Ogawa, and N. Kondo, Robotics **2**, 36 (2013).
25) B. Quintana, S. A. Prieto, and A. Adán, Int. Conf. Indoor Positioning and Indoor Navigation, 2016.
26) J. Tiemann and C. Wietfeld, Int. Conf. Indoor Positioning and Indoor Navigation, 2017.
27) R. Hostettler and S. Särkkä, Int. Conf. Indoor Positioning and Indoor Navigation, 2016.
28) Y. Norose, K. Mizutani, and N. Wakatsuki, Jpn. J. Appl. Phys. **51**, 07GB17 (2012).
29) Y. Norose, K. Mizutani, and N. Wakatsuki, Jpn. J. Appl. Phys. **53**, 07KC19 (2014).
30) K. Kakuma, Y. Norose, K. Mizutani, and N. Wakatsuki, Jpn. J. Appl. Phys. **52**, 07HC10 (2013).
31) R. Miyamoto, K. Mizutani, T. Ebihara, and N. Wakatsuki, Jpn. J. Appl. Phys. **54**, 07HC11 (2015).
32) R. Miyamoto, K. Mizutani, T. Ebihara, and N. Wakatsuki, Jpn. J. Appl. Phys. **55**, 07KC06 (2016).
33) R. Miyamoto, K. Mizutani, T. Ebihara, and N. Wakatsuki, Jpn. J. Appl. Phys. **56**, 07JC09 (2017).
34) A. Osumi, T. Saito, and Y. Ito, Jpn. J. Appl. Phys. **54**, 07HC07 (2015).
35) A. Osumi, M. Ogita, K. Okitsu, and Y. Ito, Jpn. J. Appl. Phys. **56**, 07JC12 (2017).
36) K. Mizutani, K. Nishizaki, K. Nagai, and K. Harakawa, Jpn. J. Appl. Phys. **36**, 3176 (1997).
37) K. Mizutani, K. Itoga, K. Kudo, L. Okushima, and N. Wakatsuki, Jpn. J. Appl. Phys. **43**, 3090 (2004).
38) Y. Katano, N. Wakatsuki, and K. Mizutani, Jpn. J. Appl. Phys. **48**, 07GB03 (2009).
39) I. Saito, N. Wakatsuki, K. Mizutani, M. Ishii, L. Okushima, and S. Sase, Jpn. J. Appl. Phys. **47**, 4329 (2008).
40) I. Saito, K. Mizutani, and N. Wakatsuki, Jpn. J. Appl. Phys. **46**, 4537 (2007).
41) N. Wakatsuki, S. Kinjo, J. Takarada, and K. Mizutani, Jpn. J. Appl. Phys. **49**, 07HC14 (2010).
42) H. Nishiguchi, T. Sawayama, and K. Nagamune, Jpn. J. Appl. Phys. **55**, 07KB05 (2016).
43) H. Iwaya, K. Mizutani, T. Ebihara, and N. Wakatsuki, Jpn. J. Appl. Phys. **56**, 07JC07 (2017).